



**HAL**  
open science

## Low temperature grown GaNAsSb: A promising material for photoconductive switch application

Kian Hua Tan, Sonn Fatt Yoon, Satrio Wicaksono, Wan Khai Loke, D. S. Li, Naïma Saadsaoud, Charlotte Tripon-Canseliet, Jean-Francois Lampin, Didier Decoster, Jean Chazelas

► **To cite this version:**

Kian Hua Tan, Sonn Fatt Yoon, Satrio Wicaksono, Wan Khai Loke, D. S. Li, et al.. Low temperature grown GaNAsSb: A promising material for photoconductive switch application. Applied Physics Letters, 2013, 103 (11), pp.111113. 10.1063/1.4820797 . hal-00861768

**HAL Id: hal-00861768**

<https://hal.sorbonne-universite.fr/hal-00861768v1>

Submitted on 27 May 2022

**HAL** is a multi-disciplinary open access archive for the deposit and dissemination of scientific research documents, whether they are published or not. The documents may come from teaching and research institutions in France or abroad, or from public or private research centers.

L'archive ouverte pluridisciplinaire **HAL**, est destinée au dépôt et à la diffusion de documents scientifiques de niveau recherche, publiés ou non, émanant des établissements d'enseignement et de recherche français ou étrangers, des laboratoires publics ou privés.

# Low temperature grown GaNAsSb: A promising material for photoconductive switch application

Cite as: Appl. Phys. Lett. **103**, 111113 (2013); <https://doi.org/10.1063/1.4820797>

Submitted: 02 June 2013 • Accepted: 25 August 2013 • Published Online: 12 September 2013

K. H. Tan, S. F. Yoon, S. Wicaksono, et al.



View Online



Export Citation



CrossMark

## ARTICLES YOU MAY BE INTERESTED IN

[GaNAsSb material for ultrafast microwave photoconductive switching application](#)

Applied Physics Letters **93**, 063509 (2008); <https://doi.org/10.1063/1.2971204>

[Influence of surface passivation on ultrafast carrier dynamics and terahertz radiation generation in GaAs](#)

Applied Physics Letters **89**, 232102 (2006); <https://doi.org/10.1063/1.2398915>

[Band parameters for III-V compound semiconductors and their alloys](#)

Journal of Applied Physics **89**, 5815 (2001); <https://doi.org/10.1063/1.1368156>

Lock-in Amplifiers  
up to 600 MHz



Zurich  
Instruments



## Low temperature grown GaNAsSb: A promising material for photoconductive switch application

K. H. Tan,<sup>1</sup> S. F. Yoon,<sup>1</sup> S. Wicaksono,<sup>1</sup> W. K. Loke,<sup>1</sup> D. S. Li,<sup>1</sup> N. Saadsaoud,<sup>2</sup>  
 C. Tripon-Canseliet,<sup>2</sup> J. F. Lampin,<sup>3</sup> D. Decoster,<sup>3</sup> and J. Chazelas<sup>4</sup>

<sup>1</sup>*School of Electrical and Electronic Engineering, Nanyang Technological University, Nanyang Avenue, Singapore 639798, Republic of Singapore*

<sup>2</sup>*Laboratoire d'Electronique et Electromagnétisme, Pierre and Marie Curie University, 4 Place Jussieu, 75005 Paris, France*

<sup>3</sup>*Institute of Electronics, Microelectronics and Nanotechnology (IEMN), UMR CNRS 8520,*

*Université des Sciences et Technologies de Lille, BP 60069, 59652 Villeneuve d'Ascq Cedex, France*

<sup>4</sup>*Thales Airborne Systems, 2 Avenue Gay Lussac, 78852 Elancourt, France*

(Received 2 June 2013; accepted 25 August 2013; published online 12 September 2013)

We report a photoconductive switch using low temperature grown GaNAsSb as the active material. The GaNAsSb layer was grown at 200 °C by molecular beam epitaxy in conjunction with a radio frequency plasma-assisted nitrogen source and a valved antimony cracker source. The low temperature growth of the GaNAsSb layer increased the dark resistivity of the switch and shortened the carrier lifetime. The switch exhibited a dark resistivity of  $10^7 \Omega \text{cm}$ , a photo-absorption of up to 2.1  $\mu\text{m}$ , and a carrier lifetime of  $\sim 1.3$  ps. These results strongly support the suitability of low temperature grown GaNAsSb in the photoconductive switch application. © 2013 AIP Publishing LLC. [<http://dx.doi.org/10.1063/1.4820797>]

The photoconductive switch has attracted interest due to its potential application in terahertz optoelectronics. An ideal photoconductive switch has a photo absorption layer, which has short carrier lifetime, a high dark electrical resistivity, and high quantum efficiency. A high dark resistivity ensures good electrical isolation when the switch is off. A short carrier lifetime improves the switch performance at a high frequency. Furthermore, a short carrier lifetime ( $< 1$  ps) is also an essential requirement to generate a sub-picosecond electrical pulse in terahertz applications. High quantum efficiency enhances the photo-responsivity of a switch to the incoming light signal.

The photoconductive switch has been demonstrated using low temperature grown GaAs (LT-GaAs). LT-GaAs based photoconductive switches operate at wavelengths of shorter than 880 nm and exhibit the characteristics of a high dark electrical resistivity, good carrier mobility, and an ultra-short carrier lifetime. In the LT-GaAs photoconductive switch module, Ti:sapphire lasers are usually used as the photon excitation source.<sup>1</sup> The wavelength of a Ti:sapphire laser ranges between 650 nm and 1100 nm. It operates most efficiently at 800 nm, closely matched to the band gap energy of LT-GaAs. In addition, the Ti-sapphire laser is complicated in design and bulky in size. These characteristics of the Ti-sapphire laser constrain the usability of the LT-GaAs-based photoconductive switch.

Research efforts towards the photoconductive switch operated at a wavelength of 1.55  $\mu\text{m}$  have gained attention due to the possibility of using an inexpensive and maintenance-free pulsed 1.55  $\mu\text{m}$  Er: fiber laser system. Compared to the Ti-sapphire laser, the 1.55  $\mu\text{m}$  Er: fiber laser offers advantages regarding stability, simplicity, and compactness. Furthermore, the abundance of availability of the cheap 1.55  $\mu\text{m}$  Er: fiber laser due to its popularity in telecommunication applications is another advantage for switching

to the 1.55  $\mu\text{m}$  photoconductive switch system. Due to the bandgap energy of 1.42 eV in LT-GaAs, the quantum efficiency of the LT-GaAs photoconductive switch at a wavelength of 1.55  $\mu\text{m}$  is profoundly low due to insufficient photon absorption. The LT-GaAs could absorb a 1.55  $\mu\text{m}$  photon only by utilizing a trap-assisted two-step photon absorption process,<sup>2</sup> which is not a band-to-band absorption process. Tani *et al.*<sup>3</sup> have reported that the detection efficiency of LT-GaAs at 1.55  $\mu\text{m}$  is only 10% of its detection efficiency at 780 nm. There was an effort to improve the performance of LT-GaAs photoconductive coupled with fiber laser using a frequency doubled fiber laser.<sup>4</sup> The wavelength of the 1.55  $\mu\text{m}$  fiber laser is converted to 780 nm using non-linear optics to enhance the photon absorption in LT-GaAs. Alternatively, a material, which has an energy bandgap of  $< 0.8$  eV is required in the 1.55  $\mu\text{m}$  photoconductive switch application to produce a sufficient photo-response.

$\text{In}_{0.53}\text{Ga}_{0.47}\text{As}$  is an obvious choice for the 1.55  $\mu\text{m}$  photoconductive switch applications due to its band gap energy of 0.74 eV. However,  $\text{In}_{0.53}\text{Ga}_{0.47}\text{As}$  has a low dark electrical resistivity and a long carrier lifetime. To counter these shortcomings, a variation of  $\text{In}_{0.53}\text{Ga}_{0.47}\text{As}$ , such as low temperature grown InGaAs (LT-InGaAs)<sup>5-7</sup> and ion-irradiated InGaAs<sup>8</sup> have also been reported. Both results<sup>7,8</sup> showed a reduced sub-picosecond (0.9 ps) carrier lifetime. However, both LT-InGaAs and ion-irradiated InGaAs exhibited a low dark electrical resistivity value of  $< 3 \Omega \text{cm}$ ,<sup>7,9</sup> which is detrimental to the performance of the photoconductive switch. Hatem *et al.*<sup>10</sup> have demonstrated the application of a Fe-doped InGaAs-based photoconductive switch in terahertz application. The Fe-doped InGaAs exhibited an ultra-narrow electrical pulse (0.6 ps in FWHM) and a dark resistivity of up to  $2.2 \times 10^3 \Omega \text{cm}$ .

An ErAs:InGaAs superlattices structure<sup>11,12</sup> was also reported in 1.55  $\mu\text{m}$  photoconductive switch applications. It

used ErAs islands as efficient carrier traps to shorten the carrier lifetime of the material. With the assistance of compensating Be doping, the ErAs:InGaAs superlattices were capable of exhibiting a dark resistivity of  $3.43 \times 10^2 \Omega \text{ cm}$ .

Another alternative, a InGaAs/InAlAs multi-layer structure,<sup>13</sup> was also demonstrated in the  $1.55 \mu\text{m}$  photoconductive switch application. A thin ( $\sim 10 \text{ nm}$ ) LT-InGaAs layer was sandwiched by two InAlAs layers in the InGaAs/InAlAs multi-layer structure. The deep trap levels in the InAlAs layers captured the residual photo-generated carrier from the LT-InGaAs layer, leading to a high dark resistivity of  $10^6 \Omega \text{ cm}$  in the switch. Due to the thin photo-absorption LT-InGaAs layer,  $>100$  periods of InGaAs/InAlAs layers were needed to produce sufficient quantum efficiency.

In our previous report,<sup>14</sup> we demonstrated the suitability of the GaNAsSb material in the photoconductive switch application. In a separate report,<sup>15</sup> we also demonstrated the application of the GaNAsSb-based photoconductive switch in microwave signal switching. In these reports, the GaNAsSb-based photoconductive switch was shown to have a dark resistivity of  $\sim 1500 \Omega \text{ cm}$  and a carrier lifetime of  $>30 \text{ ps}$ . The GaNAsSb material also exhibited a photo-response up to  $1.6 \mu\text{m}$ . Further improvement in the performance of the GaNAsSb-based photoconductive switch is needed to increase its dark resistivity and shorten its carrier lifetime.

In this letter, we report a performance improvement in the GaNAsSb-based photoconductive switch by utilizing low temperature grown GaNAsSb (LT-GaNAsSb) as the active material. The dark electrical resistivity and carrier lifetime of the LT-GaNAsSb are measured. The photo-absorption spectra and the photo-response of the LT-GaNAsSb material are also presented.

To fabricate the photoconductive switch, two samples with a layer structure as shown in Fig. 1 were grown using molecular beam epitaxy in conjunction with a radio frequency (RF), plasma-assisted nitrogen source, and a valved antimony cracker source. Both a GaAs buffer layer and a  $1 \mu\text{m}$ -thick LT-GaNAsSb layer were grown at  $200^\circ\text{C}$ . In the first sample, sample A, the LT-GaNAsSb layer contained  $\sim 5.0\%$  of nitrogen and  $\sim 12\%$  of Sb. In the second sample, sample B, the LT-GaNAsSb layer contained  $\sim 4.5\%$  of nitrogen and  $\sim 12\%$  of Sb. Compared to our previous reports,<sup>14,15</sup> the content of N in the GaNAsSb layer was increased from  $3.5\%$  to  $4.5\text{--}5.0\%$  to achieve a smaller bandgap in the

material. The increase in N content also helped to reduce the compressive strain in the layer as it had a smaller lattice mismatch.

The composition of N and Sb in each sample was independently determined using a (004) rocking curve X-ray diffraction (XRD) measurement. The determination of N and Sb composition using the (004) rocking curve in quaternary materials, such as GaNAsSb, is more complicated because it involves two unknown variables: the composition of N atoms and the composition of Sb atoms. Thus, a calibration sample was needed to determine the composition of N and Sb prior to growth of the device samples containing the GaNAsSb material.

The calibration sample consisted of a  $50 \text{ nm}$ -thick GaAsSb layer and followed by a  $200 \text{ nm}$ -thick GaNAsSb layer. The composition of Sb atoms in both layers was first determined by fitting the rocking curve of the GaAsSb layer. Since the Sb flux was kept unchanged during the growth of the GaAsSb and GaNAsSb layers, it is expected that both layers contain roughly equal amount of Sb. Using the value of Sb composition in the GaAsSb layer, the composition of N atoms in the GaNAsSb layer can be determined by fitting the rocking curve of the GaNAsSb layer. The detail description of this XRD measurement process can be found elsewhere.<sup>16</sup>

The presence of arsenic antisite defects in the dilute nitride materials such as GaNAs, InGaAsN, and GaNAsSb has been reported in various studies.<sup>17–22</sup> The formation of arsenic antisite defects in the dilute nitride material is likely due to their low growth temperature ( $<500^\circ\text{C}$ ), compared to the growth temperature of low defect GaAs ( $580^\circ\text{C}$ ). Chen *et al.*<sup>18</sup> have reported that the concentration of the arsenic antisite defects in the dilute nitride material increases in response to the decrease in the growth temperature of the dilute nitride material. This is consistent with the findings that higher concentration of arsenic antisite defects in the GaAs grown at lower temperature. Our previous report<sup>14</sup> showed that the GaNAsSb material, which was grown at  $400^\circ\text{C}$ , exhibited a dark resistivity of  $\sim 1500 \Omega \text{ cm}$  and a carrier lifetime of  $>30 \text{ ps}$ . This value of resistivity and carrier lifetime is clearly insufficient for the high performance photoconductive switch application. Higher arsenic antisite concentration in the material is needed to shorten the carrier lifetime and increase the resistivity.

In this study, the growth temperature of the LT-GaNAsSb layer was reduced to  $200^\circ\text{C}$  to increase the As antisite defects in the layer. Arsenic antisite defects acted as efficient mid-gap carrier recombination centers, resulting in a high resistivity and a short carrier lifetime in the material. After growth, the samples were *in situ* annealed at  $600^\circ\text{C}$  for  $15 \text{ min}$  under As overpressure.

Photoconductive switches with an electrode were fabricated using the standard photolithography process. These electrodes consisted of two  $150 \mu\text{m} \times 150 \mu\text{m}$  Pt( $100 \text{ \AA}$ )/Ti( $300 \text{ \AA}$ )/Pt( $100 \text{ \AA}$ )/Au( $3000 \text{ \AA}$ ) contact pads, which were deposited on the LT-GaNAsSb active layer. These contacts were subjected to a  $45 \text{ s}$  rapid thermal annealing process at  $450^\circ\text{C}$ .

The dark electrical resistivity of both samples was measured using a contactless Hall effect measurement. In sample

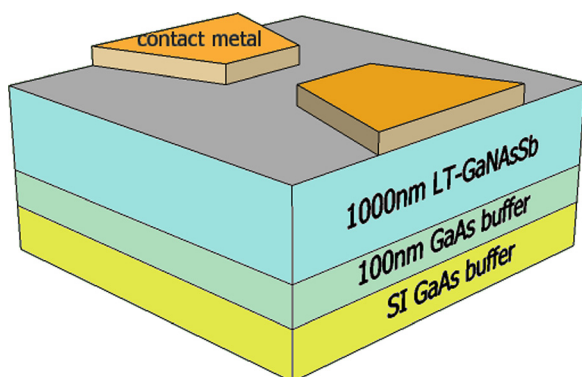


FIG. 1. Schematic diagram of the LT-GaNAsSb-based photoconductive switch.

A (with 5.0% of N), the measured resistivity was  $\sim 1 \times 10^7 \Omega \text{ cm}$ . In sample B (with 4.5% of N), the measured resistivity was  $\sim 2 \times 10^7 \Omega \text{ cm}$ . These values of resistivity are comparable to the resistivity of LT-GaAs, and it is significantly higher than the resistivity of the other reported  $1.55 \mu\text{m}$  photoconductive switches mentioned earlier. The high resistivity in LT-GaAs could be likely due to the high density of the As antisite defect, leading to a dominating carrier-hopping conduction mechanism in the layer.<sup>23,24</sup> Hall measurement also showed a carrier mobility of  $\sim 6 \text{ cm}^2/\text{V s}$  and  $\sim 12 \text{ cm}^2/\text{V s}$  in sample A and sample B, respectively. This value is low compared to carrier mobility in LT-GaAs, which has a value of  $\sim 2000 \text{ cm}^2/\text{V s}$ .

The optical transmission of the sample was measured using a Fourier transform spectrometer and near-infrared quartz as the light source. The measured optical transmission of both samples is shown in Fig. 2. The absorption coefficient  $\alpha$  can be extracted from transmission results using the Beer-Lambert law  $I = I_0 e^{-\alpha x}$ , where  $I$  and  $I_0$  are the output and incident light intensity, respectively.  $x$  is the layer thickness. The extracted absorption coefficient of both samples is also shown in Fig. 2. From Fig. 2, it can be seen that  $\sim 20\%$  of the incident light at a wavelength of  $1.5 \mu\text{m}$  was absorbed by the GaNAsSb-based photoconductive switch in sample A. In sample B, only  $\sim 7\%$  of the incident light at a wavelength of  $1.5 \mu\text{m}$  was absorbed. Figure 2 showed that  $\alpha$  has a value of  $\sim 2000 \text{ cm}^{-1}$  and  $\sim 900 \text{ cm}^{-1}$  at  $1.55 \mu\text{m}$  for sample A and sample B, respectively. Furthermore, both samples also showed a photo-absorption up to a wavelength of  $2.1 \mu\text{m}$ . This is the longest cut-off wavelength ever reported in GaAs-based dilute nitride material. The photoresponsivity of GaNAsSb at  $1.55 \mu\text{m}$  was measured by comparing the output power of the switch between the ON state and the OFF state. In this measurement, a  $1 \text{ W}$   $1.55 \mu\text{m}$  laser was used as an excitation light source to turn on the switch. The switch on sample A showed a  $25 \text{ dB}$  increase in the output power when it was switched on.

The carrier lifetime of the switch was measured using time-resolved optical transmission at room temperature. The

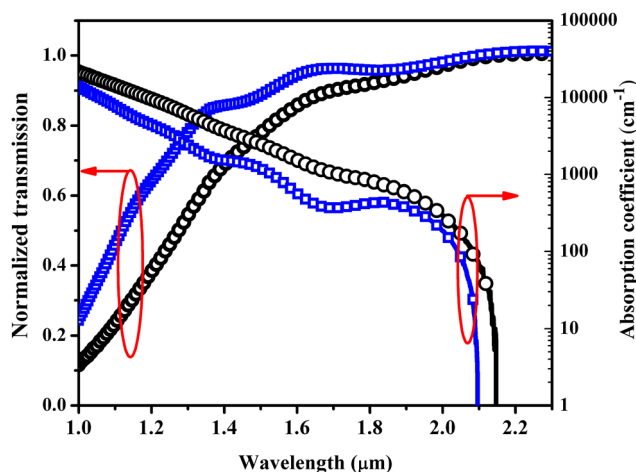


FIG. 2. Plot of optical transmission spectra and absorption coefficient of the LT-GaNAsSb vs. wavelength. Black circle (O) symbol represents sample A, which contained 5.0% of N and 12% of Sb. Blue square (□) symbol represents sample B, which contained 4.5% of N and 12% of Sb in GaNAsSb layer.

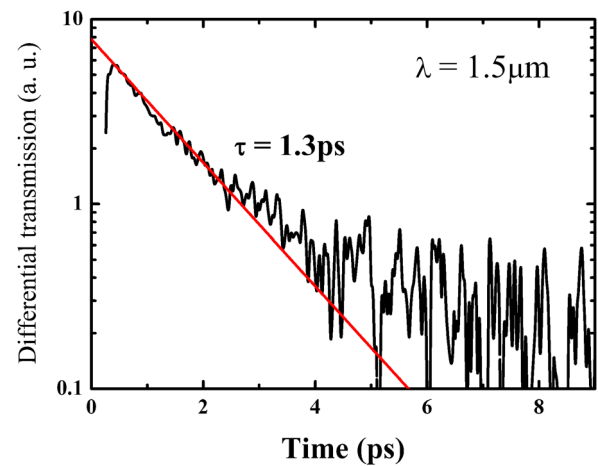


FIG. 3. Normalized differential transmission curve of LT-GaNAsSb-based photoconductive switch on sample A with 5.0% of N and 12% of Sb in the GaNAsSb layer. Red line is a fitted exponential decay curve using  $\tau = 1.3 \text{ ps}$ .

optical excitation source in the measurement was a  $1.55 \mu\text{m}$  optical parametric oscillator with a pulse FWHM of  $150 \text{ fs}$ , which was synchronously pumped by a mode-locked tunable titanium-sapphire laser. The power of incident light per pulse was  $25 \mu\text{J cm}^{-2}$  in the measurement. The transmitted light was measured by an InGaAs photodetector coupled with a lock-in amplifier. The measured normalized differential transmission curve of sample A is shown in Fig. 3. The carrier lifetime of the switch can be extracted by fitting the time constant of the exponential decay curve in the figure. LT-GaNAsSb in sample A exhibited a carrier lifetime of  $1.3 \text{ ps}$ , much shorter compared to that of normal GaNAsSb. Due to weaker photon absorption at  $1.55 \mu\text{m}$  in sample B, the response of sample B in the time-resolved optical transmission measurement using a  $1.55 \mu\text{m}$  optical parametric oscillator was extremely weak. Thus, a  $1.3 \mu\text{m}$  optical parametric oscillator was used to measure the carrier lifetime of the switch in sample B. The measured normalized differential transmission curve of sample B at  $1.3 \mu\text{m}$  is shown in Fig. 4. It can be seen that sample B exhibited a carrier

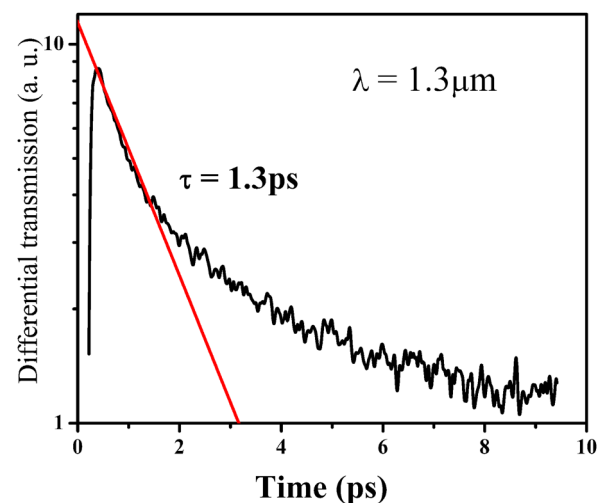


FIG. 4. Normalized differential transmission curve of LT-GaNAsSb-based photoconductive switch on sample B with 4.5% of N and 12% of Sb in the GaNAsSb layer. Red line is a fitted exponential decay curve using  $\tau = 1.3 \text{ ps}$ .



lifetime of  $\sim 1.3$  ps, which is similar to the carrier-lifetime observed in sample A. The results of carrier lifetime from both samples clearly showed that lowering the growth temperature of GaNAsSb has been very effective in shortening the carrier lifetime of the material as it promotes the formation of mid-gap recombination centers such as arsenic anti-site defects.

In conclusion, the LT-GaNAsSb-based photoconductive switch has been demonstrated with an improved performance. A dark resistivity of  $\sim 1 \times 10^7 \Omega \text{ cm}$  has been achieved, which exceeds the dark resistivity reported in previous  $1.55 \mu\text{m}$  photoconductive switches. The switch is capable of absorbing light with a wavelength up to  $2.1 \mu\text{m}$ . LT-GaNAsSb also exhibited a short carrier lifetime of  $\sim 1.3$  ps, making it a promising material for  $1.55 \mu\text{m}$  photoconductive switch application.

This work was supported by A\*STAR under SERC Grant No. 102 167 0116. Pierre and Marie Curie University and IEMN further acknowledge support by the ANR under Grant No. ANR-10-INTB-0908-CERISE. We gratefully acknowledge the assistance of Thales Airborne System in this study.

- <sup>1</sup>C. Wood, J. Cunningham, I. C. Hunter, P. Tosch, E. H. Linfield, and A. G. Davies, *Int. J. Infrared Millim. Waves* **27**(4), 557 (2006).  
<sup>2</sup>H. Erlig, S. Wang, T. Azfar, A. Udupa, H. R. Fetterman, and D. C. Streit, *Electron. Lett.* **35**(2), 173 (1999).  
<sup>3</sup>M. Tani, K.-S. Lee, and X. C. Zhang, *Appl. Phys. Lett.* **77**(9), 1396 (2000).  
<sup>4</sup>S. Kasai, T. Katagiri, J. Takayanagi, K. Kawase, and T. Ouchi, *Appl. Phys. Lett.* **94**(11), 113505 (2009).  
<sup>5</sup>H. Kunzel, J. Bottcher, R. Gibis, and G. Urmann, *Appl. Phys. Lett.* **61**(11), 1347 (1992).  
<sup>6</sup>J. P. Ibbetson, J. S. Speck, A. C. Gossard, and U. K. Mishra, *Appl. Phys. Lett.* **62**(18), 2209 (1993).

- <sup>7</sup>S. Gupta, J. F. Whitaker, and G. A. Mourou, *IEEE J. Quantum Electron.* **28**(10), 2464 (1992).  
<sup>8</sup>J. Mangeney, L. Joulaud, P. Crozat, J. M. Lourtioz, and J. Decobert, *Appl. Phys. Lett.* **83**(26), 5551 (2003).  
<sup>9</sup>N. Chimot, J. Mangeney, L. Joulaud, P. Crozat, H. Bernas, K. Blary, and J. F. Lampin, *Appl. Phys. Lett.* **87**(19), 193510 (2005).  
<sup>10</sup>O. Hatem, J. Cunningham, E. H. Linfield, C. D. Wood, A. G. Davies, P. J. Cannard, M. J. Robertson, and D. G. Moodie, *Appl. Phys. Lett.* **98**(12), 121107 (2011).  
<sup>11</sup>K. K. Williams, Z. D. Taylor, J. Y. Suen, H. Lu, R. S. Singh, A. C. Gossard, and E. R. Brown, *Opt. Lett.* **34**(20), 3068 (2009).  
<sup>12</sup>F. Ospald, D. Maryenko, K. von Klitzing, D. C. Driscoll, M. P. Hanson, H. Lu, A. C. Gossard, and J. H. Smet, *Appl. Phys. Lett.* **92**(13), 131117 (2008).  
<sup>13</sup>B. Sartorius, H. Roehle, H. Kunzel, J. Bottcher, M. Schlak, D. Stanze, H. Venghaus, and M. Schell, *Opt. Express* **16**(13), 9565 (2008).  
<sup>14</sup>K. H. Tan, S. F. Yoon, C. Tripon-Canseliet, W. K. Loke, S. Wicaksono, S. Faci, N. Saadsaoud, J. F. Lampin, D. Decoster, and J. Chazelas, *Appl. Phys. Lett.* **93**(6), 063509 (2008).  
<sup>15</sup>K. H. Tan, C. Tripon-Canseliet, S. Faci, A. Pagies, M. Zegaoui, W. K. Loke, S. Wicaksono, S. F. Yoon, V. Magnin, D. Decoster, and J. Chazelas, *IEEE Photon. Technol. Lett.* **22**(15), 1105 (2010).  
<sup>16</sup>S. Wicaksono, S. F. Yoon, K. H. Tan, and W. K. Cheah, *J. Cryst. Growth* **274**(3-4), 355 (2005).  
<sup>17</sup>W. K. Loke, S. F. Yoon, K. H. Tan, S. Wicaksono, and W. J. Fan, *J. Appl. Phys.* **101**(3), 33122 (2007).  
<sup>18</sup>W. M. Chen, I. A. Buyanova, C. W. Tu, and H. Yonezu, *Physica B* **376-377**, 545 (2006).  
<sup>19</sup>S. Y. Xie, S. F. Yoon, and S. Z. Wang, *J. Appl. Phys.* **97**(7), 73702 (2005).  
<sup>20</sup>S. Tanaka, A. Moto, M. Takahashi, T. Tanabe, and S. Takagishi, *J. Cryst. Growth* **221**(1-4), 467 (2000).  
<sup>21</sup>N. Q. Thinh, I. A. Buyanova, P. N. Hai, W. M. Chen, H. P. Xin, and C. W. Tu, *Phys. Rev. B* **63**(3), 033203 (2001).  
<sup>22</sup>K. H. Tan, S. Wicaksono, W. K. Loke, D. Li, S. F. Yoon, E. A. Fitzgerald, S. A. Ringel, and J. S. Harris, Jr., *J. Cryst. Growth* **335**(1), 66 (2011).  
<sup>23</sup>D. C. Look, D. C. Walters, M. O. Manasreh, J. R. Sizelove, C. E. Stutz, and K. R. Evans, *Phys. Rev. B* **42**(6), 3578 (1990).  
<sup>24</sup>D. C. Look, *J. Appl. Phys.* **70**(6), 3148 (1991).